Journal Pre-proofs

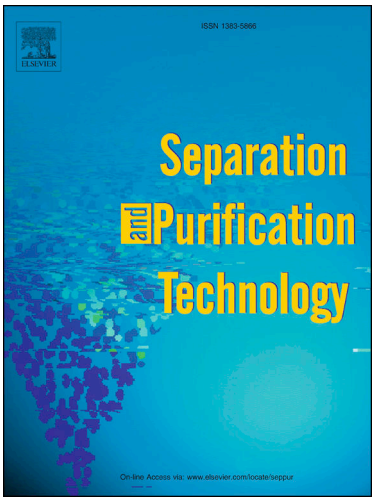

Modelling and simulation of hollow fiber membrane vacuum regeneration for CO_2 desorption processes using ionic liquids

Jose Manuel Vadillo, Daniel Hospital-Benito, Cristian Moya, Lucia Gomez-Coma, Jose Palomar, Aurora Garea, Angel Irabien

PII: S1383-5866(21)01173-4
DOI: https://doi.org/10.1016/j.seppur.2021.119465
Reference: SEPPUR 119465

To appear in: *Separation and Purification Technology*

Received Date: 26 April 2021
Revised Date: 29 July 2021
Accepted Date: 8 August 2021

Please cite this article as: J. Manuel Vadillo, D. Hospital-Benito, C. Moya, L. Gomez-Coma, J. Palomar, A. Garea, A. Irabien, Modelling and simulation of hollow fiber membrane vacuum regeneration for CO_2 desorption processes using ionic liquids, *Separation and Purification Technology* (2021), doi: https://doi.org/10.1016/j.seppur.2021.119465

Modelling and simulation of hollow fiber membrane vacuum regeneration for CO_2 desorption processes using ionic liquids.

Jose Manuel Vadillo[a*], Daniel Hospital-Benito[b], Cristian Moya[b], Lucia Gomez-Coma[a], Jose Palomar[b], Aurora Garea[a], Angel Irabien[a].

[a] *Chemical and Biomolecular Engineering Department. Universidad de Cantabria.39005 Santander. Spain.*

[b] *Chemical Engineering Department. Universidad Autónoma de Madrid. 28049 Madrid. Spain.*

**Correspondence: vadillojm@unican.es*

Abstract

A novel modelling and simulation framework on CO_2 desorption process from post-combustion CO_2 capture was developed by a coupled membrane vacuum regeneration technology (MVR) and four imidazolium ionic liquids (ILs) with remarkably different viscosity values. The ILs 1-ethyl-3-methylimidazolium acetate ([emim][Ac]), 1-butyl-3-methylimidazolium acetate ([bmim][Ac]), 1-butyl-3- methylimidazolium isobutyrate ([bmim][i-but]), 1-butyl-3-methylimidazolium glycinate ([bmim][GLY]) were selected. COSMO based/Aspen Plus methodology was effectively implemented to estimate the physical and chemical CO_2 absorption parameters by kinetic and thermodynamic models fitted to experimental data to design the regeneration process in Aspen Plus software. The membrane contactor unit for solvent regeneration was custom-built and successfully imported into the simulation tool, as no model library for the MVR existed yet in the commercial package for the steady state process flowsheet simulation. The effect on CO_2 desorbed flux and process performance was evaluated for the comparison purpose between ILs at different operational conditions. High temperature, vacuum level and module length are beneficial to the solvent regeneration process, while low

liquid flow-rate increases the CO_2 desorption flux but also decrease the process performance. The viscosity, CO_2 solubility and reaction enthalpy were identified as key thermodynamic properties of IL selection. The IL ([emim][Ac]) presented the highest regeneration performance (around 92% at 313 K and vacuum pressure of 0.04 bar) with a total energy consumption of 0.62 $MJ \cdot kgCO_2^{-1}$, which is lower than conventional amino-based high temperature regeneration process (1.55 $MJ \cdot kgCO_2^{-1}$). These results pointed out the interest of the membrane vacuum regeneration technology based on ILs compared to the conventional solvent-based thermal regeneration, but further techno-economic evaluation is further needed to ensure the competitiveness of this novel CO_2 desorption approach to the large-scale application.

Highlights

- Membrane vacuum regeneration (MVR) technology was studied for CO_2 desorption in carbon capture & utilization system.
- 4 Ionic liquids (ILs) with chemical absorption of CO_2 are evaluated by process analysis.
- CO_2 solubility, viscosity and molecular weight are stated as key IL properties for CO_2 desorption mass transfer.
- The MVR technology could decrease the regeneration energy consumption from 1.55 to 0.62 $MJ \cdot kgCO_2^{-1}$.

Keywords: CO_2 capture, Membrane vacuum regeneration, Ionic liquids, Process simulation, COSMO-based/Aspen Plus, Custom-built ACM/ Aspen Plus

1. Introduction

Carbon capture, utilization and sequestration (CCUS) are novel technologies used to control CO_2 emissions by various approaches, which involve the capture of CO_2 from the output gas of industrial processes to permanent storage in geological cavities (CCS) or to use as a resource for carbon-based products (CCU). The transportation of the captured is usually via pipeline or ship [1]. Carbon capture systems are usually classified into three main technologies (post-combustion, pre-combustion and oxy-fuel) depending mainly of the industrial process proposed for the implementation of this technology. For power generation plants, post-combustion CO_2-capture can be easily implemented as it can be retrofitted to existing power plants [2].

Solvent-based CO_2 capture through absorption coupled by Hollow Fiber Membrane Contactor (HFMC) technology has been considered in recent years as a promising technique for CO_2 separation processes [3]. The main advantages of HFMC technology in continuous absorption and desorption CO_2 using membrane contactors with the absorbent are the following key aspects: independent both liquid and gas flow-rates, known contact area, easy scale-up due to the modularity, and avoidance of drop dragging [4]. The membrane material is one of the most significant parameters since promotes the HFMC technology efficiency. A depth analysis of the state of the art has been developed in a previous work [5]. In addition, recent works studied the future direction in membrane materials and selection criteria [6]. To summarize, up to date the more studied membrane material used for CO_2 capture technology are ceramic or polymeric with a membrane pore size lower than 200 nm, due to greater pore size could lead absorbent penetration, which sharply reduce the mass transfer of CO_2 through the membrane.

On the one hand, microporous ceramic membranes, such as zeolites, silica or alumina could take advantage due to their chemical and thermal resistance. Nevertheless, up to date, there are important drawbacks and bottle-neck for the use of ceramic membranes that have yet to be addressed in CO_2 capture technology. By comparison with polymeric membranes, the ceramic membranes have lower CO_2 selectivity and permeability, higher cost and lower contact area/volume.

On the other hand, microporous polymers, especially membranes made of polypropylene (PP), polyvinylidene fluoride (PVDF), and polytetrafluoro- ethylene (PTFE), are predominantly employed in CO_2 capture systems mainly due to their commercial availability, low cost, versatility and hydrophobic nature [7]. However, some membrane contactor issues such as wetting phenomena and fouling must be avoided due to the increase of the CO_2 mass transfer resistance [5]. Moreover, since the desorption stage normally needs elevated temperature, a major challenge is the membrane stability. For this purpose, membrane vacuum regeneration technology (MVR) has been recently suggested [8–11]. The application of vacuum for CO_2 desorption lowering the solvent regeneration temperature and the corresponding energy consumption to the overall CO_2 capture system. Decreasing the regeneration temperature would also contribute significantly to increase the applicability of low-cost polymeric membranes[12]. In this work we use for calculations a commercial polymeric HFMC due to its hydrophobicity, low-cost production, commercial availability and wide range of chemical and morphological tunability [9].

Alkanolamines are the most typical used absorbents for carbon capture process using HFMC, specifically monoethanolamine (MEA), mainly due to the low-cost, low viscosity and high CO_2 absorption, even at low CO_2 partial pressures. However, several drawbacks have been

documented for amine-based CO_2 capture, such as an energy intensive regeneration for the desorption of CO_2, high absorbent loss, degradability and corrosiveness of the HFMC [13]. In order to address these deficiencies, ionic liquids (ILs) have been recently presented as promising absorbents alternative for coupled CO_2 capture with membrane technology [14]. The ILs are molecular structures consisting of cations and anions, and special functional groups, which provide outstanding properties, such as negligible vapor pressure, tunable structure, high thermal and chemical stability, high CO_2 affinity, and low energy demand for regeneration [15].

Some research studies that focused in CO_2 absorption process by coupled HFMC technology and ILs, were pointed out as follows: Dai et al. [16] and Bai et al. [17] studied the CO_2 absorption capacity of ILs with physical and chemical interactions by experimental data using HFMC technology; Gomez-Coma et al. [18,19] analyzed the temperature and water content influence on imidazolium ILs 1-ethyl-3-methyl-imidazolium ethyl sulfate [Emim][EtSO4] and ILs 1-ethyl-3-methyl-imidazolium acetate[emim][Ac]; Albo et al. [20] evaluated the non-dispersive absorption of CO_2 into the same ILs using different HFMC configuration (parallel- and cross-flow); Martins et al. [21,22] proposed a chemisorption and absorption dynamics model for CO_2 absorption on HFMC by novel biocompatible cholinium lysinate IL; Mulukutla et al. [23] and Bazhenov et al. [24] focused on the ionic liquid-membrane compatibility and the performance of the coupled absorption-desorption system; Lu et al. [25], Simons et al. [26] and Qazi et al. [27–29] covered some aspects of design, modelling and experimental set-up for coupled absorption-desorption process using different ILs, focusing on the absorption performance increase due to the desorption process, and concluding that chemical ILs led to higher CO_2 loading capacity even at atmospheric pressure while physical ILs were able to be fully regenerated.

Nevertheless, there is a lack of studies focused on the modelling and simulation of the CO_2 desorption by HFMC using ILs, even though the desorption stage is responsible for most energy consumption in Post-combustion CCUS. For this purpose, a custom 2D model for the CO_2 desorption process by membrane vacuum regeneration (MVR) using the IL [emim][Ac] was developed in a previous research work [9]. The model was created with Aspen Custom Modeler (ACM) software. By means of a sensibility analysis of Henry constant, it was concluded that more efforts should be focused to the IL properties estimation. To contribute to the CO_2 desorption process by HFMC in the CCUS scheme with ILs, more research on process simulation could be helpful for designing/selection ILs as absorbents with optimized properties for CO_2 capture process, taking into account the extra degree of freedom in ILs design provided by the tunability property [30]. For this purpose, two issues have to be solved:

(i) Although there are various studies that present rigorous modeling approaches for CO_2 capture by HFMC technology and ILs, by using different mathematical programming or computational fluid dynamics software tools, the model library of the most common commercial process simulation tools, such as Aspen Plus (AP), does not have implemented any process unit of HFMC for the CO_2 desorption simulation, as a non-dispersive gas-liquid contactor. Therefore, a 2D mathematical model, developed using Aspen Custom Modeler (ACM) in our previous work [9], to study the CO_2 desorption using HFMC technology in a MVR configuration was integrated/exported as an ACM custom model into AP environment and validated with experimental results of the CO_2 steady state desorption process, using the data

of [emim][Ac] previously reported [9] as the selected IL reference (Supplementary Material, Figure S1).

(ii) Some ILs are not included in the commercial process simulators database, as they are not conventional chemical compounds. Therefore, ILs have to be defined as non-databank compounds which some information for estimating the unknown properties of both, pure ILs and (CO_2-ILs) mixture, are required. Conventional thermodynamic models used in simulation tools for absorbent properties estimation, such as the equation of state (EOS), molecular simulations and activity coefficient models based on group contribution method (GCM), have several computational problems such as the large experimental data requirements, scarce vapor-pressure data, unknown critical properties and complex parameter estimation due to the non-volatile behavior of the ILs, which leads to a practical limitation for design and/or select ILs with competitive properties for CO_2 capture technology [31–33]. For this reason, developing more advanced models were required for the phase behaviors estimation at different thermodynamic conditions for ILs. Some of these novel modeling techniques, already used in absorption-desorption process, are both, artificial intelligence [31–33] and predictive quantum methods [34], such as Adaptive Neuro-Fuzzy Inference System (ANFIS) and Conductor-like Screening Model for Real Solvents (COSMO-RS), respectively.

In this work, a COSMO-RS method has been proposed recently as a completely new perspective to understand the CO_2 capture since the thermodynamic properties of both, pure ILs and CO_2-ILs mixture, are predicted using only structural data of the molecules [35]. This provides greater flexibility for screening appropriate ILs

based on calculations, without fully depends on experimental data [36]. In order to combine this novel method of property estimation with simulation and optimization tasks, previous research was focused to the integration of the COSMO-based methodologies and the commercial simulation tool Aspen Plus by COSMOSAC property model, which is used to create and/or specify the new non-databank IL components by using the results generated from COSMO-RS calculations [37].

Considering these challenges on the CO_2 capture system by coupled HFMC technology and ILs, the aim of this work is to develop a new simulation framework in CO_2 desorption by MVR process with ILs, focusing on the custom-built model integration into a commercial simulation tool (Aspen Plus) by using COSMOSAC property method for the prediction of both, pure IL and CO_2-IL mixtures properties. For this purpose, the physical and chemical CO_2 absorption parameters (viscosity, equilibrium and Henry's constants) using in AP software, were estimated by kinetic and thermodynamic models fitted to experimental data (CO_2 solubility and solvent viscosity) at different temperatures.

Summarizing the aim of the present study, we used a COSMO based/Aspen Plus methodology in order to (i) define both physical and chemical CO_2 absorption parameters using AP software, (ii) simulate the CO_2 desorption process by coupled HFMC technology and ILs using a custom 2D model developed in ACM due to the lack of HFMC unit operation in the simulation tool Aspen Plus. The ILs analyzed were 1-ethyl-3-methylimidazolium acetate ([emim][Ac]), 1-butyl-3-methylimidazolium acetate ([bmim][Ac]), 1-butyl-3-methylimidazolium isobutyrate ([bmim][i-but]), 1-butyl-3-methylimidazolium glycinate ([bmim][GLY]) (Supplementary Material, Table S1). We assumed the approach in which the

experiments and simulations are limited to the CO_2 desorption process while the absorbent circulation and the absorption stage were not evaluated. The effects of permeate side pressure, temperature, liquid flow-rate and the HFMC length on the regeneration efficiency and CO_2 desorbed mole-flow were analyzed, and the most appropriate operational conditions in terms of the energy consumption are compared to other referenced works to study the feasibility of using coupled HFMC technology and ILs as alternative of conventional CO_2 absorbents.

2. Methodology

In order to understand the importance of the COSMO-based/Aspen Plus approach in the conceptual design of new CO_2 desorption process based on ILs, this section briefly covers information about: (i) the computational details for IL property prediction by COSMO-RS calculations to define the COSMOSAC property method (in code 1) for Aspen Plus simulations [37]; (ii) the integration, into the AP simulation tool, of the custom HFMC model created for the IL regeneration process in a carbon capture system; (iii) and the energy consumption terms of the CO_2 desorption process at different operational conditions.

2.1. Computational details

2.1.1. Component definition and property method

The CO_2 desorption process was modeled employing the commercial process simulator Aspen Plus v11 in order to set a framework for further simulations of CO_2 desorption by both HFMC technology and ILs. Following a COSMO-based/Aspen Plus methodology, the pure IL and the CO_2-IL reaction products were introduced into AP by the COSMOSAC property method (with code 1) as non-databank pseudo component [37]. The complete procedure carried out to include

new non-databank compounds into Aspen Plus and to run simulations entailing them was described in detail by Palomar et al. [37]. As summary, figure 1 shows the information flow diagram used for COSMO-based/Aspen Plus methodology from microscale to macroscale approaches. A conceptual parametric flow diagram for the modelling and simulation based on this COSMO-RS and Aspen Plus approach were detailed in figure S2 of Supplementary Material.

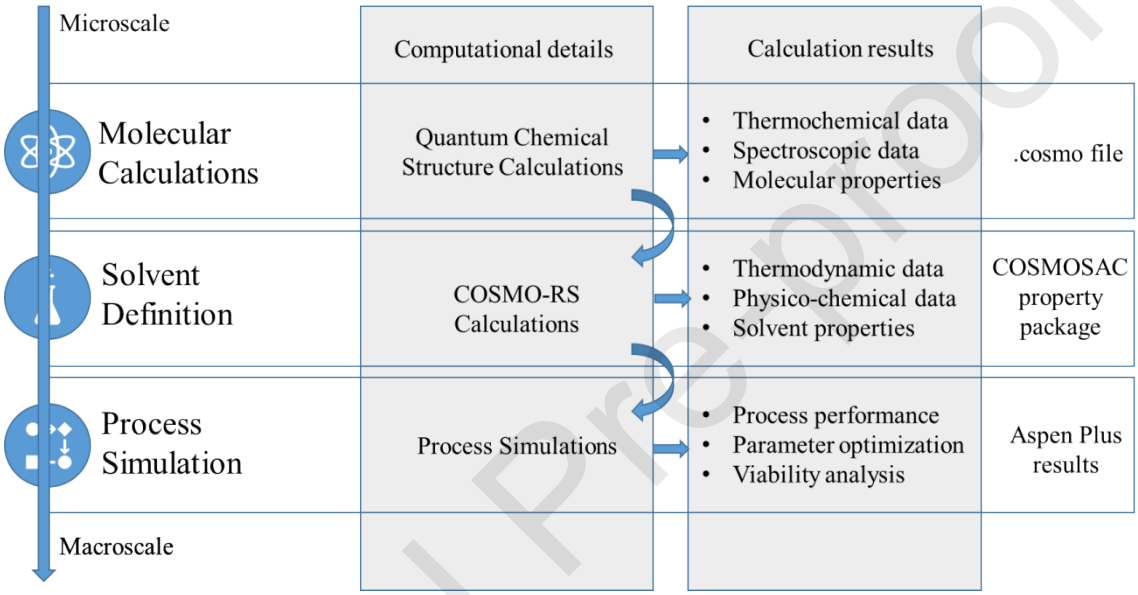

Figure 1. Multi-scale COSMO-based/Aspen Plus methodology. Computational flow diagram.

The following procedures were needed to specify the thermophysical properties (required for the COSMOSAC property method) of the molecules calculated.

(i) Quantum chemical structure calculations, which predict the distribution of polarized charge on the molecular surface (σ-Surface) of both, ILs and reaction products, as a result of the molecular geometry optimization process at BP-TZVP computational level. A .cosmo file was created from the molecular geometry optimization, which store the ideal screening charges on the molecular surface computed by the COSMO

methodology. The quantum-chemical calculations and the .cosmo file generation were carried out by Turbomole 4.5 software. This information was then used as an input file for COSMO-RS calculations.

(ii) COSMO-RS calculations, which adapt the molecular geometry information (.cosmo file) into usual thermodynamic data. These thermodynamic properties required in the COSMOSAC Property Model Specification for further simulation, were used in the IL pseudo-component creation. All COSMO-RS calculations were performed by COSMOtherm program v.19 with parametrization BP_TZVP_C30_1201. In this work, the properties estimated as a result of COSMO-RS calculations, as can be seen in Table S2 of supplementary material, are mainly molecular weight, density, normal boiling point, molecular volume, σ-profile.

Additionally, to better describe thermodynamic and kinetic model, which describe the capacity of ILs to absorb CO_2, experimental data at different temperatures were used in Aspen Plus software to the calculation of both equilibrium and Henry's constant and viscosity. For IL [emim][Ac], which was not been previously evaluated by COSMO-based/Aspen Plus methodology, the experimental viscosity and solubility values at different temperatures were reported by Zareiekordshouli et al. [38] and Shiflett and Yokozeki [39], respectively. For the other ILs evaluated in this work ([bmim][Ac], [bmim][GLY] and [bmim][i-but]), the experimental data were taken from the previously published work of Hospital-Benito et al. [30].

The experimental data of the ILs viscosity at different temperatures were fitted to the form of Andrade equation (eq. 1), and added into the Aspen Properties for the CO_2 mass transfer kinetics estimation.

$$Ln\,\mu = A + \frac{B}{T} \quad (1)$$

Then, taking into account that the reaction between CO_2 and each IL studied is described as 1:2 stoichiometry (2 IL + CO_2 ↔ PROD), the experimental isotherms of these ILs were fitted to the thermodynamic model equation (Eq.2) proposed in previous work [30] where z is the absorption molar ratio ($molCO_2 \cdot molIL^{-1}$), K_H is the CO_2 Henry's constant (bar), P_{CO_2} is the CO_2 partial pressure (bar) and Keq is the CO_2-IL reaction equilibrium constant.

$$z = \frac{P_{CO_2}}{K_H - P_{CO_2}} + \frac{-2K_{eq}\frac{P_{CO_2}}{K_H} + \sqrt{K_{eq}\frac{P_{CO_2}}{K_H}}}{1 - 4K_{eq}\frac{P_{CO_2}}{K_H}} \quad (2)$$

The Keq of CO_2-IL reaction was estimated at different temperatures from (Eq. 2) and fitted to the Aspen Plus equilibrium constant equation (Eq. 3) in order to calculate the AP parameters to describe the chemical absorption.

$$Ln\,Keq = A + \frac{B}{T} \quad (3)$$

As shows (Eq. 2), the absorption of CO_2 into the IL was described using Henry's constant (K_H). The predicted K_H from the experimental isotherms are described by (Eq.4).

$$Ln\,K_H = A + \frac{B}{T} \quad (4)$$

Since the Henry's constant estimated by AP (K'_H) considers the CO_2 activity coefficient (γ_{CO_2}) in the simulator definition (eq. 5), the AP Henry´s constant (K'_H) needs a correction to an adjusted Henry's constant value (K_H), which fit to the experimental solubility estimated by the

isotherms (Eq. 2). This methodology was previously reported by Hospital-Benito et al. [30]. Experimental data used to define both the viscosity and the CO_2-IL solubility in AP were collected in figure S3 and figure S4 of Supplementary Material, respectively.

$$X_{CO_2} = \frac{P_{CO_2}}{K'_H \cdot \gamma_{CO_2}} \quad (5)$$

The diffusion coefficients and the desorption kinetics have been calculated considering the HFMC geometry and introduced by the user in Aspen Plus. The estimation of diffusion coefficients was performed by the equation proposed by Morgan et al. [40]. The enhancement factor (E) described an improvement in the mass transfer due to the reversible chemical reaction. The E factor was calculated from the experimental data of our previous work by using an optimization solver (NL2SOL) was in a good agreement with literature [9].

Both physical and chemical properties calculated by COSMO-based/Aspen Plus methodology are shown in Table 1. All the parameters used in the calculation of this properties are described in table S3 of Supplementary Material.

Table 1. Physical and chemical properties of selected IL estimated by COSMO-based/Aspen Plus approach at 313K and 1 bar: molar weight (MW), density (ρ), viscosity (μ), Henry (K_H) and reaction equilibrium (Keq) constant.

Ionic liquid	**MW ($g \cdot mol^{-1}$)**	**ρ ($kg \cdot m^{-3}$)**	**μ (mPa·s)**	**K_H (Mpa)**	**Keq**	**Reference**
[emim][Ac]	170.21	1118	42.65	10.59	89.67	This work
[bmim][Ac]	198.26	1030	179.79	9.31	65.56	[30]
[bmim][i-but]	226.32	1010	198.02	13.57	25.40	[30]
[bmim][GLY]	213.28	1030	423.87	18.06	6.78	[30]

2.1.2. Process simulation

Most simulation works on the CO_2 capture were focused on the CO_2 absorption stage while very limited research studies covered the CO_2 desorption process. Commonly, the ILs regeneration unit consists of a flash evaporator in adiabatic conditions where the CO_2 is desorbed from the IL at low pressure (0.1 bar) and high temperature (100 ºC), which required larger size operation units and high energy consumption [30,41]. The advantages to add HFMC technology into commercial simulator such AP, which demonstrate the potential in both solvent regeneration and heat recovery integration [42], will provide a tool for the overall process simulation, design and optimization. A review of the literature [43] indicated that there are no studies of CO_2 desorption using HFMC technology in a commercial simulation software that describe the HFMC unit characteristics. Therefore, the end-user has no possibility to simulate and optimizes the HFMC operation unit using the simulation tools available in the market. However, the possibility to import a user model from Aspen Custom Modeler (ACM) to the simulation software Aspen Plus, makes Aspen Tech an alternative for developers to model HFMC technology not only in laboratory scale, but also on industrial applications. From this consideration, following the Aspen Tech guideline and the multiscale COSMO-based/Aspen Plus methodology, we imported the membrane contactor model as a custom-built HFMC model, from the ACM software to the Aspen Plus simulation package, as an ACM user model added to the palette. The experimentally-validated model for CO_2 desorption process was used [9] and the material stream type was created to connect the operation units.

The model assumptions and schematic description of the model equations and fundamentals were described in Page S2 of Supplementary Material. HFMC (DES-01) specifications and experimental carbon capture process conditions are presented in table 2 and table 3. The user could describe any custom process by simple changes in the input data (membrane contactor, process conditions).

Table 2. Hollow fiber membrane contactor (HFMC) characteristics (Liqui-Cel Membrane Contactor, Minneapolis, Minnesota, USA).

Parameter	value
Membrane Material	Polypropylene
Module i.d., d_{cont} (m)	25×10^{-3}
Fiber outside diameter, d_o (m)	3×10^{-4}
Fiber inside diameter, d_i (m)	2.2×10^{-4}
Fiber length, L (m)	0.115
Number of fibers, n	2300
Effective inner membrane area, A (m^2)	0.18
Membrane thickness, δ (m)	4×10^{-5}
Membrane pore diameter, d_p (m)	4×10^{-6}
Porosity, **ς** (%)	40
Packing factor, φ	0.39
Tortuosity, τ	2.50

Table 3. Operating conditions absorption–desorption process, laboratory scale.

Parameter/Property	Value	Unit
Volume, V	100	mL
Temperature, T	289–313	K
Flue gas flow-rate, v_g	60	$mL \cdot min^{-1}$
Liquid flow-rate, v_l	60	$mL \cdot min^{-1}$
Flue gas pressure, $P_{g,in}$	1.03	bar
Liquid pressure, $P_{l,in}$	1.31	bar
Vacuum pressure, P_v	0.04–0.5	bar

This work was focused on the steady-state CO_2 stripping simulation using HFMC technology, which is part of the absorption-desorption process main flowsheet (figure 2) as well as other operation units (e.g. heat exchanger, pump, and compressor).

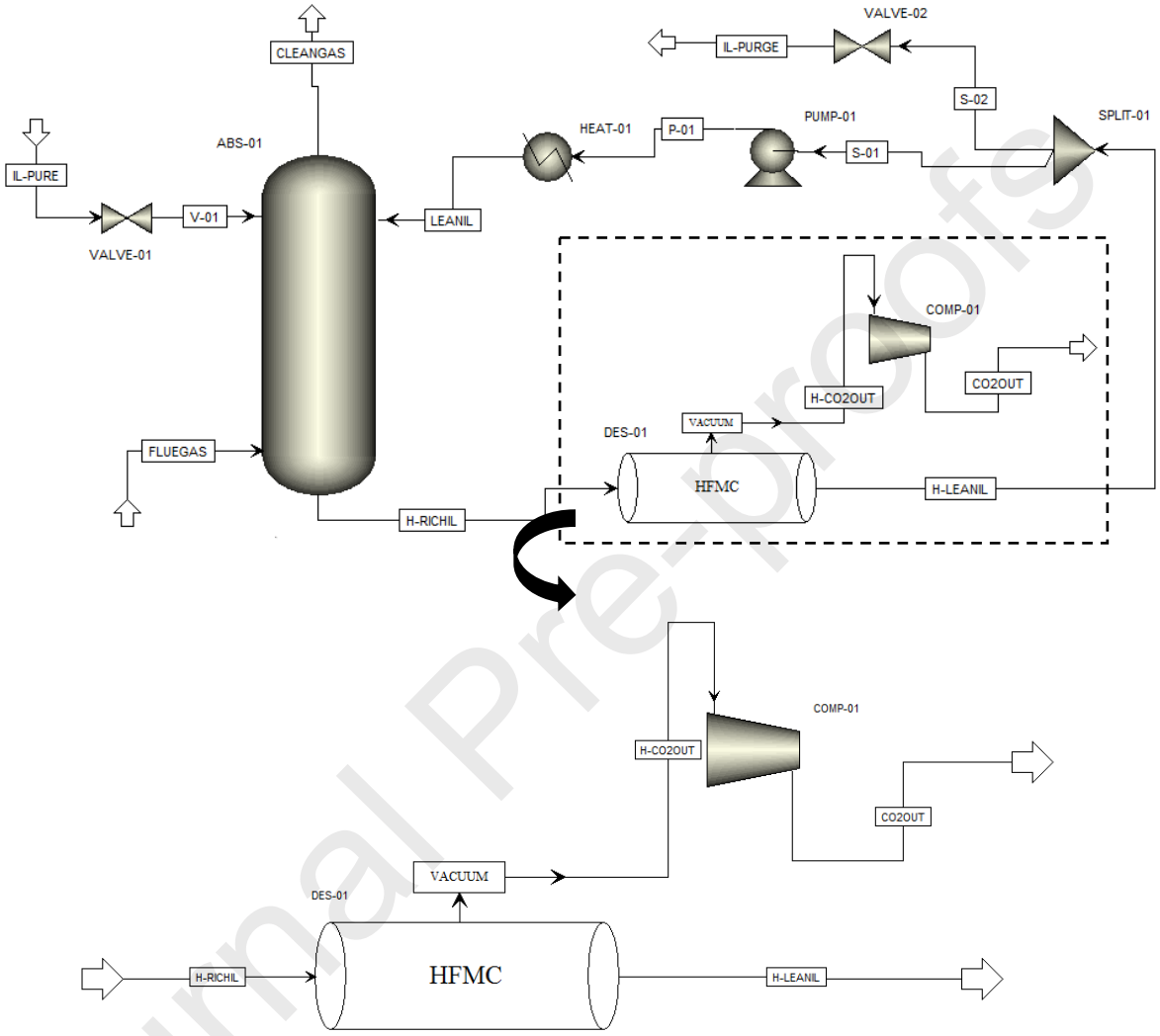

Figure 2. Continuous absorption-desorption process flowsheet in Aspen Plus software: Radfrac absorption column (ABS-01), heat exchanger (HEAT-01), liquid pump (PUMP-01), gas compressor (COMP-02), valves (VALVE-01 and VALVE-02), splitter (SPLIT-01) and membrane vacuum regeneration process (DES-01).

The imidazolium ILs evaluated in this work as absorbents present both physical and chemical CO_2 absorption and high CO_2 solubility. The operation conditions of the inlet liquid stream (H-RICHIL), which is the output of the absorption process, were defined according to (table 2). The composition of the (H-RICHIL) liquid stream was simplified to two main compounds (CO_2

absorbed into IL). The (H-RICHIL) was continuously pumped into the tube side of (DES-01), where the CO_2 was desorbed from (H-RICHIL) because of the positive effects of the vacuum pressure conditions applied in the shell side of (DES-01). The CO_2 absorbed in (H-RICHIL) exits the HFMC after its desorption (H-CO2OUT) and the regenerated IL (H-LEANIL) was recirculated to the absorption process. The CO_2 desorbed was compressed to 2 bar which was set for further CO_2 utilization [44]. In the CO_2 desorption process simulation, three main assumptions were made: (i) Steady-state and isothermal conditions; (ii) Constant concentration of IL and (iii) negligible pressure drop on the HFMC.

2.2. Energy consumption terms

To compare the HFMC technology using different absorbents in terms of energy requirements, a simplified energy consumption calculation was carried out. Moreover, the effects on the energy consumption of different operational conditions (temperature and vacuum level) were analyzed in order to decrease the consumption of energy without compromise the solvent regeneration performance.

Therefore, the total energy required to desorb CO_2 from CO_2-rich IL was calculated in this section with some general assumptions of energy calculation for HFMC desorption process by MVR:

- CO_2 desorbed from the HFMC was compressed to 2 bar, which is the output pressure of the conventional thermal regeneration process in a packing column stripper [45].
- Only the regeneration heat duty and the extra work for both vacuum pump and compression are addressed. Other operation units such as liquid pump and gas powered blower were not included.

- Compression process is isentropic.

The use of vacuum technology in CO_2 desorption process could decrease the regeneration temperature required to desorb CO_2 from the IL. Due to the lower desorption temperature for CO_2 membrane stripping than conventional thermal regeneration, therefore, it will be more reasonable to compare energy consumption with regeneration heat duty by total equivalent work [46]. Furthermore, the total energy consumption (in terms of work required) in order to remove 1 kg of CO_2, E_T ($MJ_e \cdot kgCO_2^{-1}$), is estimated in (eq. 5) as the sum of the work required for vacuum pump W_{vp}, cooling W_{cool} and compressor W_{com} ($MJ_e \cdot s^{-1}$) and the equivalent work of the regeneration heat duty W_{regen} ($MJ_e \cdot s^{-1}$) described in equation 6. Here, q_{CO_2} is the desorbed CO_2 mass-flow ($kgCO_2 \cdot s^{-1}$), Q_{regen} is the regeneration heat duty, which is the total heat required for CO_2 desorption ($MJ_{th} \cdot s^{-1}$) [47], and ξ is the energy transfer efficiency from heat to electric energy, which was assigned to a value of 0.4 [48,49].

$$E_T = \frac{(W_{vp} + W_{com} + W_{cool} + W_{regen})}{q_{CO_2}} \quad (5)$$

$$W_{regen} = \xi \cdot Q_{regen} \quad (6)$$

It must be noticed that the total energy consumption is based on the electric energy (W_i) which is represented by the abbreviation, "e", whereas the energy value of heating regeneration is based on the heat energy (Q_i) which is represented by the abbreviation, "th". So the energy transfer efficiency (ξ) was used to convert the heat energy Q_{regen} ($MJ_{th} \cdot s^{-1}$) to electric energy W_{regen} ($MJ_e \cdot s^{-1}$) in order to unitized the total energy consumption calculation E_T ($MJ_e \cdot kgCO_2^{-1}$).

The regeneration energy Q_{regen} can be further decomposed into energies required for solvent heating (sensible heat, Q_{sens}), solvent evaporation (latent heat, Q_{latent}), and CO_2 desorption (heat of reaction, Q_{rxn}), as shown in equation 7 [50,51].

$$Q_{regen} = Q_{sens} + Q_{latent} + Q_{rxn} \quad (7)$$

Since non-volatile IL was used as absorbent, the low regeneration temperature required for the MVR stripping (related to the conventional thermal regeneration processes), and the possibility of use waste heat to increase the temperature of the IL up to the regeneration step (313K, max temperature in this work), the terms of latent heat Q_{latent} and sensible heat Q_{sens} were not included in the calculations. The contribution of the regeneration energy Q_{regen} was estimated by the reaction heat Q_{rxn}, which is the desorption heat for reversing the reaction and releasing the CO_2 (eq. 8). Here, ΔH_{CO_2} (MJ_{th}·$kmolCO_2^{-1}$) is the CO_2 reaction enthalpy with IL obtained from available literature [39]; and PM_{CO_2} is the CO_2 molecular weight ($kgCO_2$ · $kmolCO_2^{-1}$)

$$Q_{regen} = Q_{rxn} = \frac{\Delta H_{CO_2}}{PM_{CO_2}} * q_{CO_2} \quad (8)$$

The following operation units were evaluated in terms of energy consumptions as follows:

The vacuum pump work requirement (W_{vp}) is estimated by (eq 9) [52], while the efficiency is expressed according to (eq 10) [53].

$$W_{vp} = \frac{G_{VP} R T Z \kappa}{(\kappa - 1)\eta_{VP}} \left[\left(\frac{P_{VP,out}}{P_{VP,in}} \right)^{\frac{(\kappa-1)}{Z\kappa}} - 1 \right] \quad (9)$$

$$\eta_{VP} = 0.1058 ln\left(\frac{P_{VP,out}}{P_{VP,in}}\right) + 0.8746 \quad (10)$$

Here, $P_{VP,in}$ is the pressure in the shell side (permeate); $P_{VP,out}$ is the atmospheric pressure. Both pressures in bar; G_{VP} is the mole-flow of the desorbed CO_2; Z is compression stage

number, and κ is the adiabatic constant. The work for the vacuum pump cooling (W_{cool}), which only depends on the (eq.9) and (eq.10) is described by Eq. (11):

$$W_{cool} = 0.054\eta_{VP}W_{VP} \quad (11)$$

The work for the compressor (W_{com}) was estimated by simulating the pressure increases in the (H-CO2OUT) from 1 to 2 bar using Aspen Plus isentropic compressor model (P-02).

At this point, the desorption by HFMC technology using ILs could be compared to that using other conventional absorbents. Moreover, the energy consumption for this novel HFMC regeneration process could be analyzed as an alternative to packed columns under an industrial context. The results of this work, presented in the following section, may contribute to identify possible additional advantages of both HFMC technology and ILs in large scale CO_2 capture plants.

3. Results and Discussion

3.1. Absorption properties

The imidazolium ILs [emim][Ac], [bmim][Ac], [bmim][GLY] and [bmim][i-but] were studied in this work for CO_2 desorption process. Both pure IL and CO_2-IL mixture properties estimated by COSMO-based/Aspen Plus approach are described in table 1 and table S3 of Supplementary Material. The considered ILs present similar densities (1010-1120 kg·m^{-3} at 313K). However, a relatively wide range of molar weight (170–230 g·mol^{-1}) and remarkably different viscosity (32-424 cP) is covered for the selected IL sample. Comparing to conventional MEA absorbent (−85 kJ·mol^{-1} at 313 K) [50,54], the heat of reaction (ΔH_R) of these ILs are remarkably low

(from -19 to -39 kJ·mol^{-1}) [55,56], which benefit both the chemical reaction reversibility and the CO_2 desorption at lower process temperatures.

The previous calculated kinetic and thermodynamic properties provided the simulation framework by Aspen Plus of the capacity of CO_2 to be absorbed by the ILs. Figure 3 shows the equilibrium isotherms at 313K obtained for the ILs studied compared to the CO_2 solubility into ILs reported by literature [30,39] to validate the property estimation by the COSMO-based/Aspen Plus methodology (see also Supplementary Material for other temperatures). At higher partial pressures (> 2 bar), the contribution of physical absorption is more relevant. However, at lower partial pressures the system is governed by chemical absorption while the contribution of physical absorption was negligible [57].

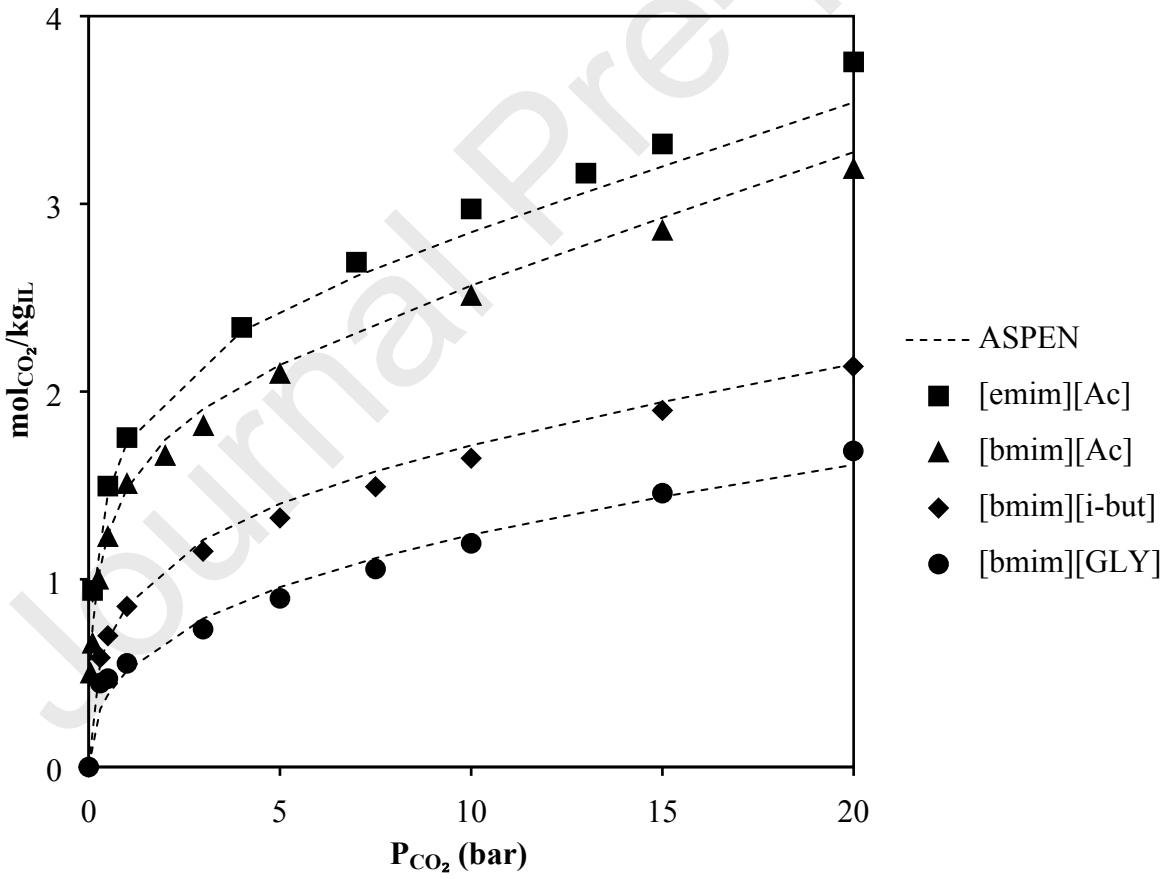

Figure 3. CO_2 absorption isotherms (Experimental vs. estimated) of 4 imidazolium ILs at 313K.

The study of these 4 imidazolium ILs is interesting because it is possible the studied of cation and anion influence on CO_2 solubility and solvent regeneration performance at same process conditions. The trend of CO_2 absorbed (in moles) into the ILs (in mass) ([emim][Ac] > [bmim][Ac] > [bmim][i-but] > [bmim][GLY]) it can be related to both favorable physical and chemical absorption, and a lower molar weight of [emim][Ac].

3.2. Regeneration process: Parametric study

Imidazolium ILs have been considered as promising solvents to absorb CO_2 and considerable experimental data of CO_2 solubility into imidazolium ILs is reported from the literature. From the base of the CO_2 solubility data, the estimation of the CO_2 desorption process performance requires more information such as the mass transfer coefficients and the contactor characteristics such as geometry and fluid dynamics [58].

Taking into account the research contribution in both areas: (i) the capability of the COSMO-RS calculations to estimate the imidazolium-based ionic liquids properties for specific anion/cations pairs [59]; and (ii) the CO_2 desorption 2D-model (developed in ACM) by HFMC using the imidazolium IL [emim][Ac] as absorbent [9], the following part of this study discusses the simulation results (the key properties of CO_2-IL systems that determines CO_2 desorption performance) of IL regeneration stage implemented in Aspen Plus as shown in figure 2.

The influence of the solvent temperature, permeate pressure, rich-CO_2 IL flow-rate and contactor length in the CO_2 desorption performance and the flux of the CO_2 desorbed through the membrane have been studied for the selected imidazolium ILs ([emim][Ac], [bmim][Ac], [bmim][GLY] and [bmim][i-but]. The base case scenario for the process conditions was chosen according to the best CO_2 desorption performance results calculated by the experimental data

of the HFMC regeneration process using [emim][Ac], which correspond to a solvent temperature of 313 K and a vacuum pressure of 0.04 bar. At this process conditions, figure 4 shows the desorption efficiency in the HFMC (Table 2, commercial contactor of laboratory scale) using the different ILs at the same operation conditions. The desorption efficiency was calculated as following:

$$\text{Desorption eff.}(\%) = \frac{\alpha_{\text{rich}} - \alpha_{\text{lean}}}{\alpha_{\text{rich}}} \text{ x } 100 \quad (12)$$

where α_{rich} and α_{lean} are the CO_2 loading in the IL $\left(\frac{mol_{CO_2}}{mol_{IL}}\right)$ before and after, respectively, of one pass of IL through the HFMC.

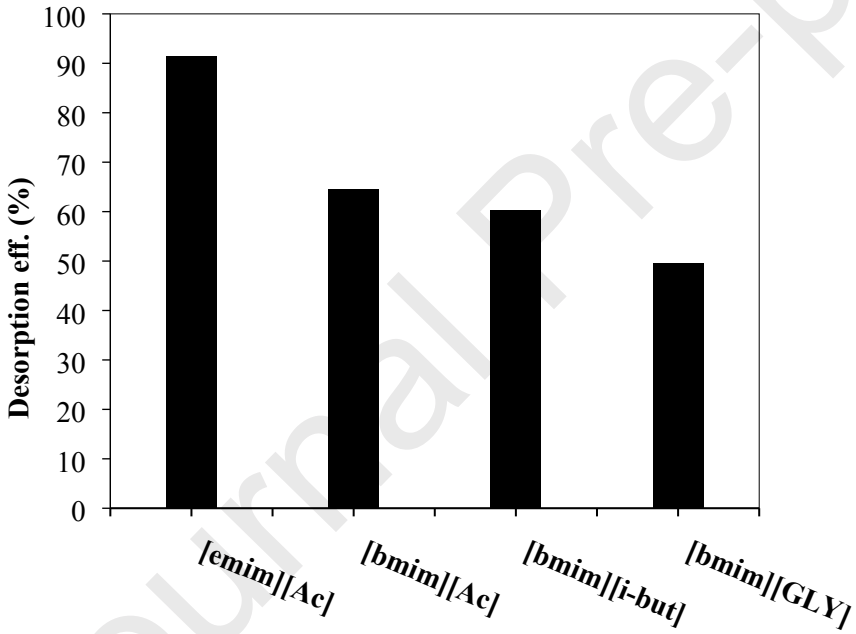

Figure 4. CO_2 desorption performance (%) in terms of ILs used at the same operational conditions in a commercial HFMC: temperature 313K, vacuum pressure 0.04 bar, liquid flow-rate 60 ml·min^{-1}.

Analyzing the trend of CO_2 desorption performance ([emim] [Ac] > [bmim][Ac] > [bmim][i-but] > [bmim][GLY]), it can be pointed out that lower viscosity (μ) increases the desorption

performance due to the increase of the CO_2 mass transfer coefficient in the ILs. Therefore, a further reduction of the energy needs to reach a target of process efficiency is possible.

The solvent temperature influence on CO_2 desorption process efficiency is shown in figure 5. The CO_2 desorption performance increases with higher solution temperature until reach the maximum desorption efficiency. If 90% desorption efficiency is considered a constraint in the simulation, the selected ILs required different temperatures to reach the performance requirement: [emim][Ac] (307 K) < [bmim][Ac] (348 K) < [bmim][i-but] (349 K) < [bmim][GLY] (356 K). This fact may be due to the lower viscosity (μ), which increases the diffusivity of CO_2 in the CO_2-rich solution since the mass transfer coefficient is controlled by liquid phase mass transfer resistance. Moreover, the CO_2 partial pressure increases at higher temperatures because of the higher concentration gradient, leading to an increase of the CO_2 desorbed mole-flow.

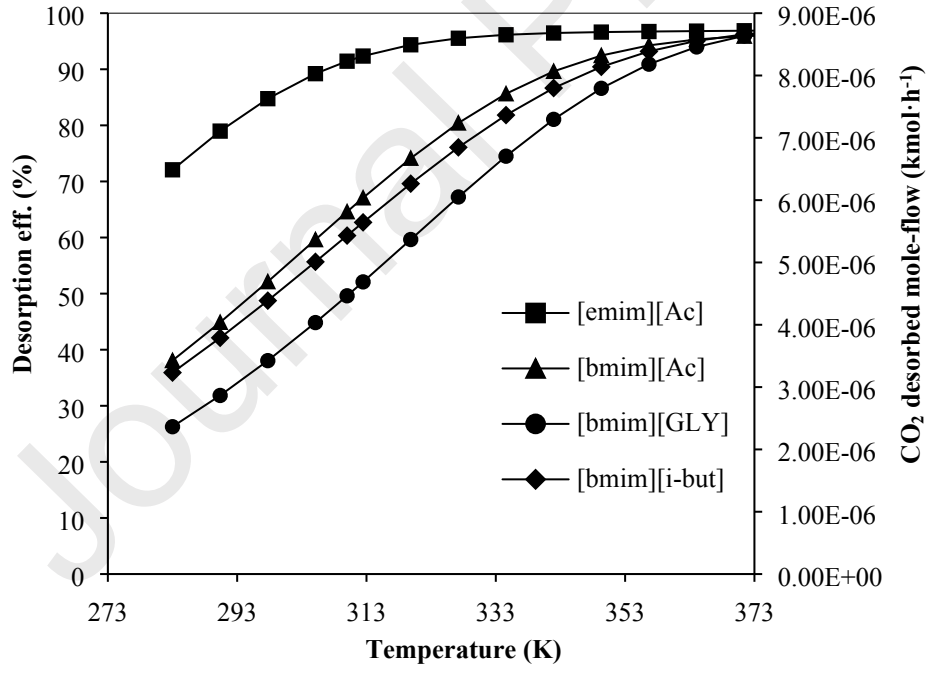

Figure 5. Desorption efficiency and CO_2 desorbed mole-flow by using 4 imidazolium ILs at different temperatures. Commercial HFMC. Operational conditions: vacuum pressure 0.04 bar, liquid flow-rate 60 ml·min^{-1}.

When varying the vacuum pressure, figure 6, low permeate pressure (higher vacuum level) enhances the process performance favoring the CO_2 mass transfer driving force through the membrane as a result of decreasing the CO_2 partial pressure in the permeate side. The CO_2 desorbed rate also increases at high vacuum level. However, low vacuum pressures increase the additional work for both the vacuum pump and compressor unit operation (discussed in section 3.3). Similar to the trend in the regeneration temperature influence, only [emim][Ac] was able to reach the process efficiency constraint (equal or higher than 90%) operating with one HFMC (module characteristics given in Table 2). Moreover, the pressure applied by the vacuum pump in the permeate side was recommended to be greater than 0.035 bar, in order to avoid wetting phenomena.

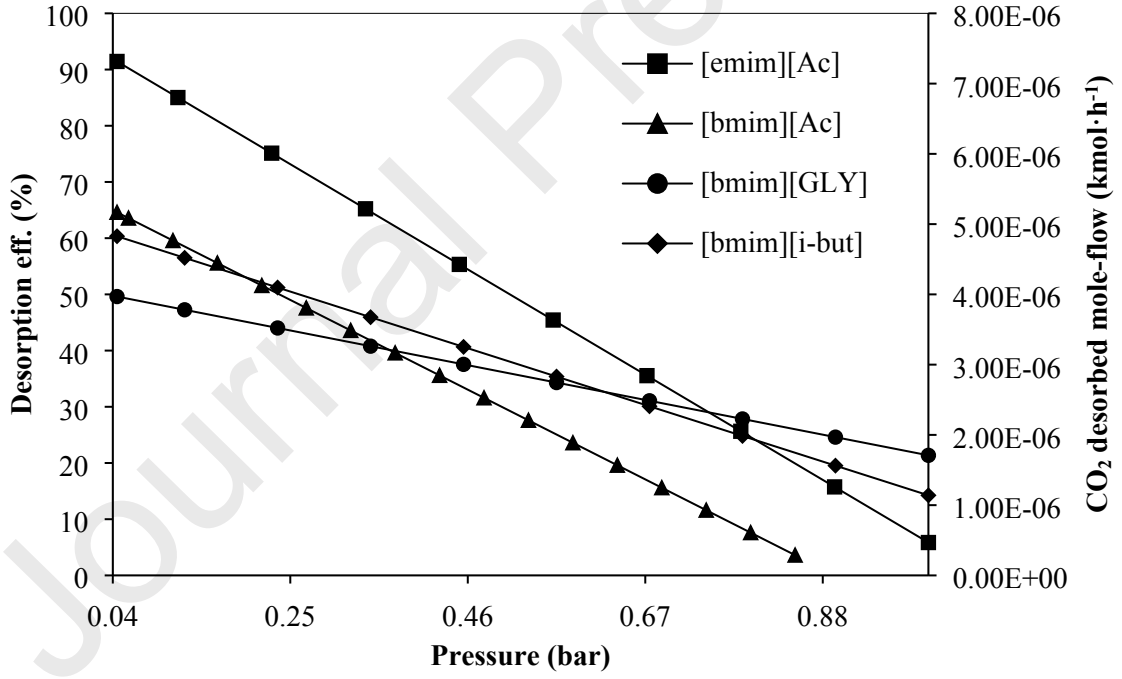

Figure 6. Desorption efficiency and CO_2 desorbed mole-flow by using 4 imidazolium ILs at different vacuum pressures. Commercial HFMC. Operational conditions: temperature 313K, liquid flow-rate 60 ml·min^{-1}.

Additionally, the CO_2-rich IL mole-flow has a negative effect on the CO_2 desorption efficiency as shown figure 7a. The reason of this poor performances at high rich solution mole-flow, could be the decrease of the residence time through the HFMC, which decrease the capacity of the CO_2 to be desorbed from the CO_2-rich IL. However, the increase of the rich solution mole-flow leads to a higher CO_2 regeneration flux as shown in figure 7b. The optimal liquid flow-rates should then be estimated by searching a trade-off between both, absorption and desorption process performances, taking into account: (i) the drawbacks of high liquid flow-rate such as the thermodynamic limitation of ILs and the risk of membrane wetting due to the increase of the liquid pressure, and (ii) the higher equipment size required associated to lower flow-rate, which increases the total capital cost of the overall process.

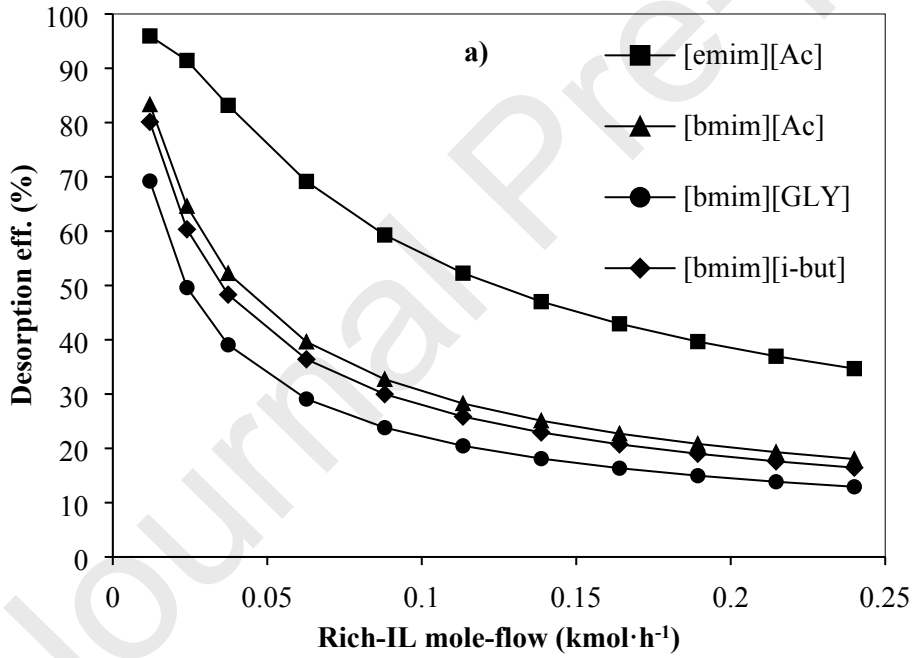

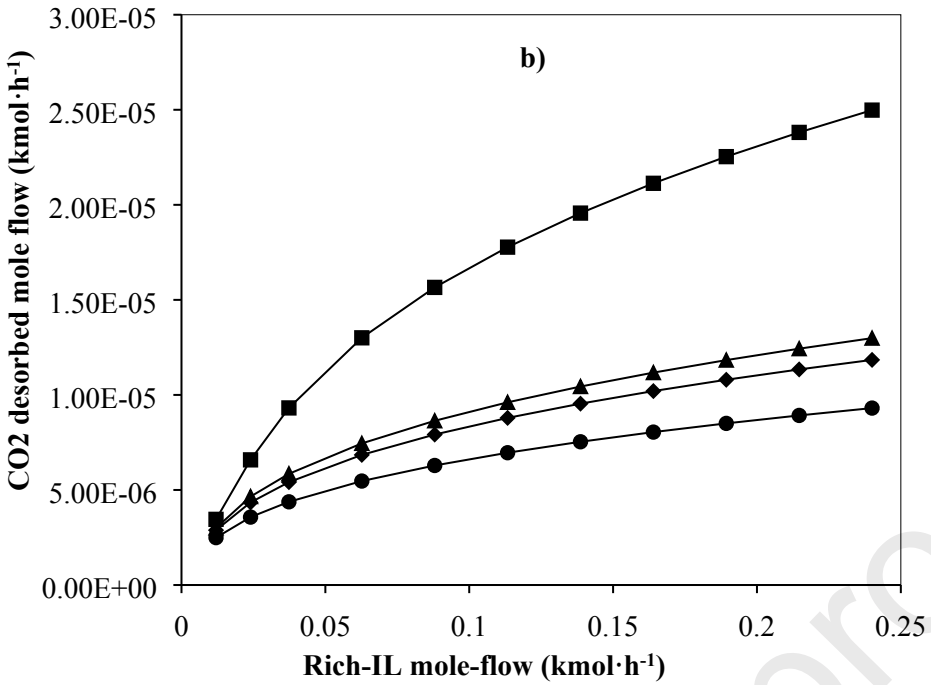

Figure 7. (a) Desorption efficiency and (b) CO_2 desorbed mole-flow by using 4 imidazolium ILs at different CO_2-rich IL mole-flow. Commercial HFMC. Operational conditions: temperature 313K, vacuum pressure 0.04 bar.

Being analyzed the operating conditions, temperature, vacuum pressure and liquid flow-rate, two more considerations that affect to the contactor could be taken into account to achieve the efficiency requirements using these ILs, [emim][Ac], [bmim][Ac], [bmim][i-but], and [bmim][GLY]: (i) Increase the number of the HFMC modules operating in series in order to increase the contact area of the desorption process; (ii) Change the materials of the HFMC in order to increase the operation temperature range.

Considering a multi-HFMC approach in the simulation task, figure 8 shows the estimation of the number of HFMCs (characteristics described in table 2) required to be operated in series to reach a CO_2 desorption efficiency of 90%. The trend on the number of HFMC required using different ILs at the same operational conditions is as follows, [emim][Ac] (1 module) < [bmim][Ac] (4 modules) < [bmim][i-but] (4 modules) < [bmim][GLY] (6 modules).

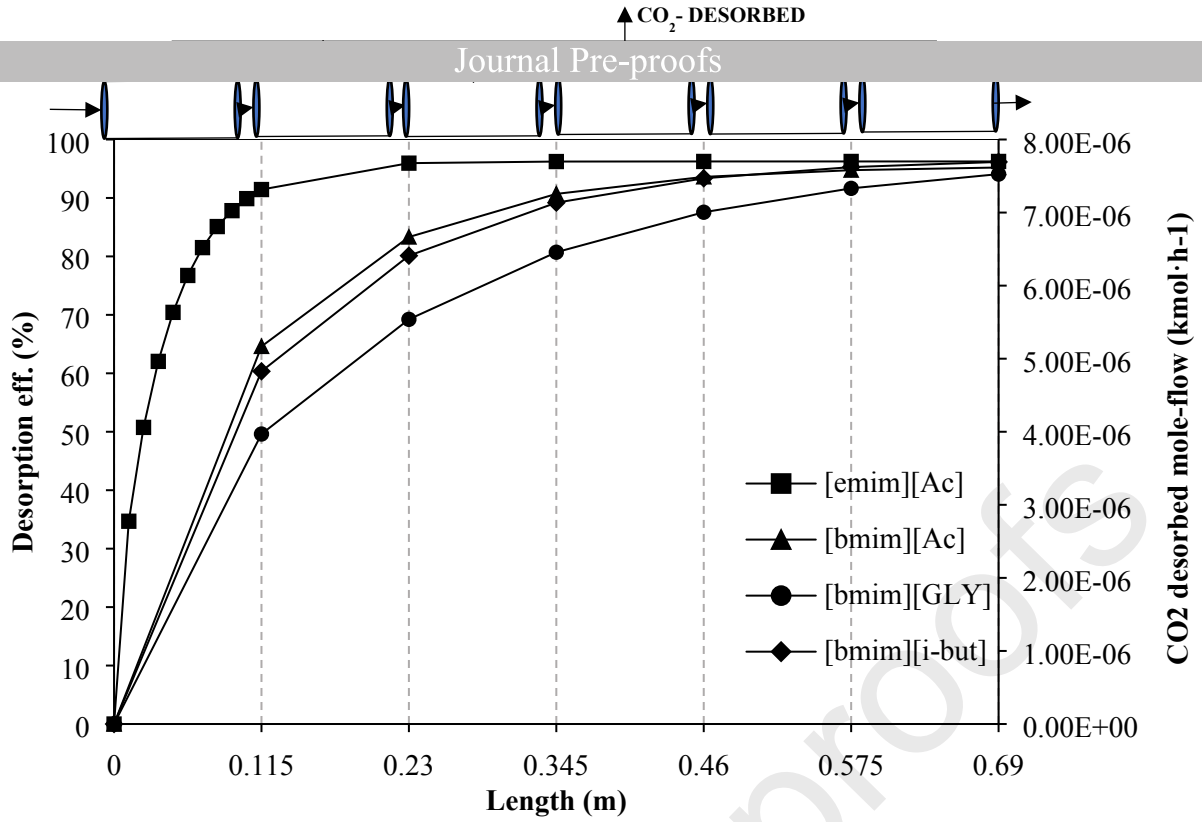

Figure 8. Desorption efficiency and CO_2 desorbed mole-flow by using 4 imidazolium ILs at different total length. Commercial HFMC modules in series. Operational conditions: temperature 313K, vacuum pressure 0.04 bar, liquid flow-rate 60 ml·min^{-1}.

3.3. Regeneration process: Energy consumption

As discussed in the Methodology section (2.2.), the CO_2 desorption process (based on MVR technology) energy requirements mainly were assumed as E_T ($MJ_e \cdot kgCO_2^{-1}$), which is the sum of (i) the work for the vacuum pump to keep the permeate side of the HFMC at low pressure conditions (W_{vp}); (ii) the energy for vacuum pump cooling (W_{cool}); (iii) the work required to compress the CO_2 desorbed from the vacuum pump output to 2 bar of pressure (W_{com}); and (iv) the desorption heat for reversing the reaction and releasing the CO_2, which is expressed by equivalent work (W_{regen}) in order to compare with the previous operational unit work terms cited. The base-operational conditions were presented in table 3, and [emim][Ac] was considered as the representative IL absorbent for the following energy consumption calculations.

The energy consumption of the MVR process at same operational parameters mainly depends on the vacuum pressure applied. Figure 9, shows the work contribution terms to the total energy of both the 3-equipment evaluated in this scheme and the regeneration heat duty converted to equivalent work, at different vacuum pressure values (0.04, 0.2 and 0.5 bar). Higher liquid temperature increases the desorbed mass-flow $\boldsymbol{q_{CO_2}}$, almost proportionally to the increase of the total work required for MVR technology, which is the sum of individual works ($\boldsymbol{W_{vp}}$, $\boldsymbol{W_{cool}}$, $\boldsymbol{W_{com}}$ $\boldsymbol{and}$ $\boldsymbol{W_{regen}}$). As result, the liquid temperature influence in the total energy consumption E_T could be depreciable. Therefore, the following energy consumption calculations (figure 9 and figure 10) have been defined for the highest temperature used in this work 313K. The comparison to room temperature calculations and the detailed energy consumption results were described in Table S3 of Supplementary Material.

As the vacuum level increases (from 0.5 to 0.04 bar), the work contribution for the vacuum pump (W_{vp}) is higher due to the additional energy to keep the permeate side at lower pressure. The work for the vacuum pump cooling (W_{cool}) depends directly of the vacuum pump energy requirements as described in equation 11. However W_{cool} only contributes 1% in the three scenarios studied in this work. The work for CO_2 desorbed stream compression (W_{com}), and the equivalent work for reversing the reaction and desorb the CO_2 at same liquid temperature (W_{regen}), are proportional to the CO_2 desorbed mole-flow (G_{VP}) as described equation 8. However, since the extent of increase in W_{vp} by increase the vacuum level, is larger than that in G_{VP} as calculated in equation 9, the contribution ratio of work ((W_{com} and W_{regen}) sharply decrease at lower P_V conditions (more vacuum level) as shown in figure 9.

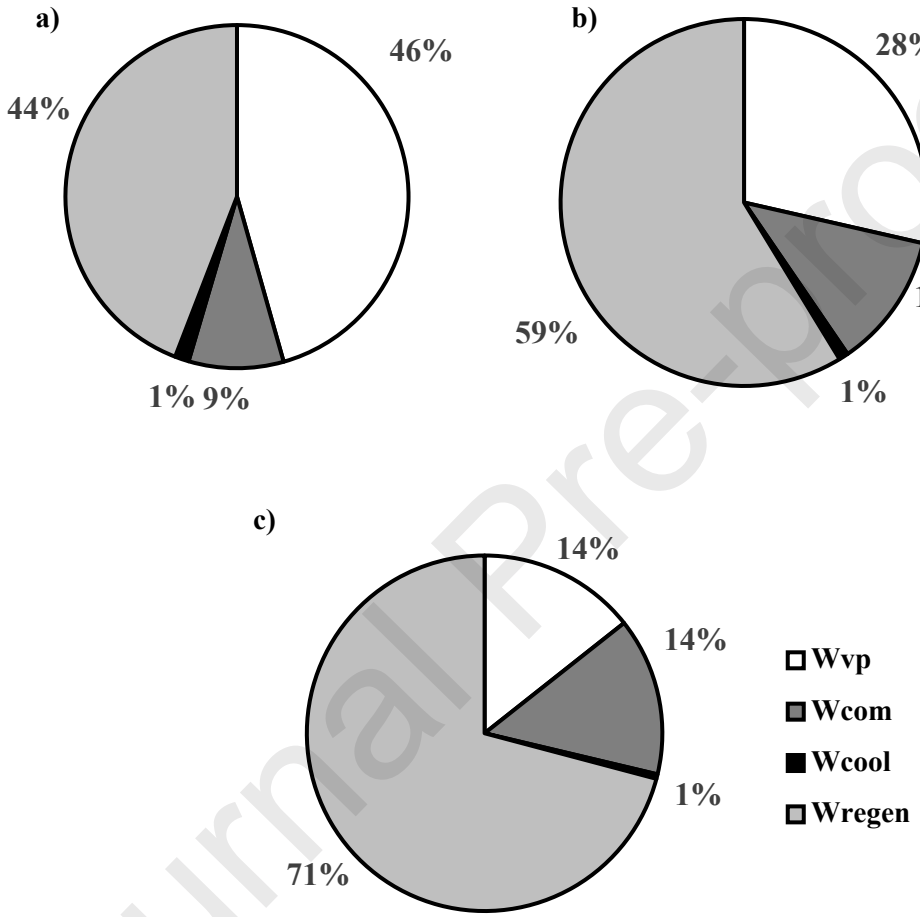

Figure 9. Percentage contribution at different conditions (to total energy consumption of the CO_2 desorption process) of the work required for vacuum pump (Wvp), compressor (Wcom), cooling of the vacuum pump (Wcool), and regeneration heat duty in terms of equivalent work (Wregen). a) vacuum pressure 0.04 bar, temperature 313K; b) vacuum pressure 0.2 bar, temperature 313K; vacuum pressure 0.5 bar, temperature 313K.

As can be seen in figure 10, the total energy consumption of the CO_2 desorption process E_T ($MJ_e \cdot kgCO_2^{-1}$), which is the sum of individually energy consumption terms (E_{vp}, E_{cool}, E_{com}

$and\ E_{regen}$), increases with higher vacuum level applied (from 0.62 to 0.34 $MJ_e \cdot kgCO_2^{-1}$). Therefore, in terms on the energy consumption, high pressure on the permeate side (low vacuum level) should be applied. However, since the desorption efficiency improves with the decrease of regeneration pressure, low vacuum level could not meet the performance requirement established for the CO_2 desorption process. One possible solution to reach the process efficiency requirements with low vacuum applied could be the increase of gas-liquid contact area (see Figure S5 of Supplementary Material). However, the process efficiency increased with a higher membrane area at different vacuum pressures until reach a constant value. Considering that, the minimum vacuum level aplied in this work in order to have a desorption efficiency equal or higher than 90% using one HFMC and [emim][Ac] as absorbent was 0.04 bar, which corresponds to a total energy consumption of 0.62 $MJ_e \cdot kgCO_2^{-1}$.

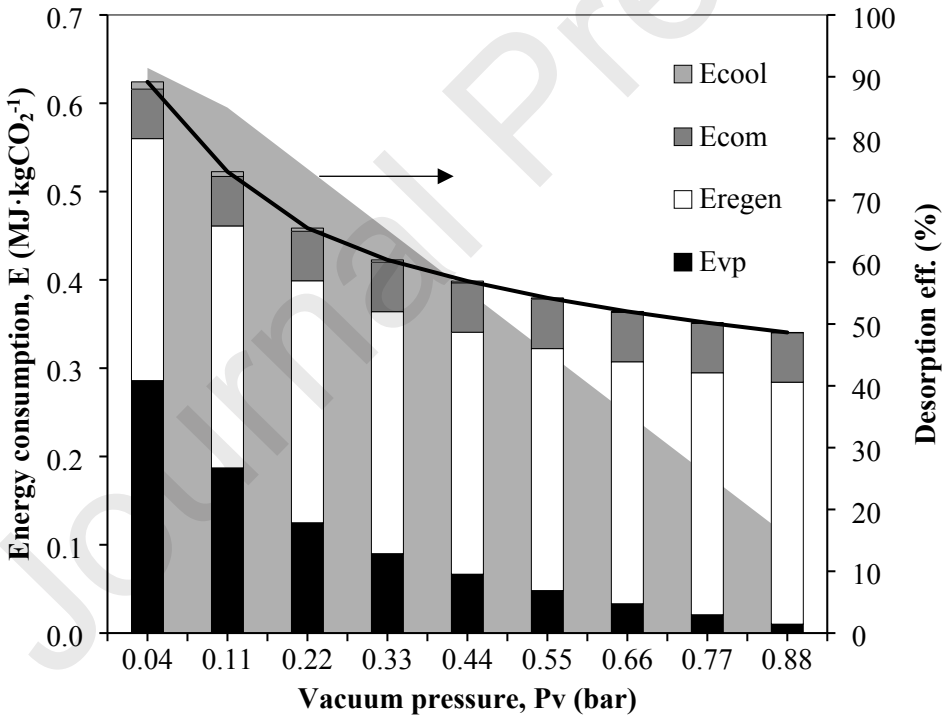

Figure 10. Total energy consumption ($MJ \cdot kgCO_2^{-1}$) and CO_2 desorption efficiency (%) at different vacuum levels and 313 K

The literature for the energy consumption of the CO_2 desorption process specifically by MVR technology are relatively scarce, being compiled in table 4 some representative studies based on energy consumption calculations. The results are limited to the solvent regeneration stage (absorption and solvent circulation are not considered) by using different absorbents and experimental conditions.

Table 4. Comparison of the total energy consumption in CO_2 desorption processes based on MVR technology.

Reference	Absorbent and method	ET ($MJ_e \cdot kgCO_2^{-1}$)
This work	Imidazolium ILs; 289-313 K; 0.04-0.88 bar	0.34-0.62
Matsumiya et al. (2005) [47]	DEA solution; 323-343 K; 0.10-0.31 bar	0.25-0.79
Yan et al. (2009) [48]	MEA solution; 308-313 K; 0.10-0.50 bar	0.5-1.6
Fang et al. (2012) [60]	MEA solution; 313-343 K; 0.10-0.48 bar	0.39-2.5
Wang et al. (2014) [45]	MEA solution; 348 K; 0.05-0.60 bar	0.78-1.4

Table 5 shows the regeneration energy consumption for conventional solvent regeneration process technology (based in a conventional flash unit or in a stripper column unit) using different absorbents, such as MEA solution, aqueous ammonia, and some representative imidazolium ionic liquids; pointing out that the efforts on new absorbent formulations, where the use of ILs as well as absorbent mixtures are being extended in further studies from the base of their tunability and functionalization options, as the recently reported studies with task specific ionic liquids (TSILs), such as aprotic heterocyclic ILs (AHA-ILs) [30,61], protic ILs (PILs) [62] and dry ILs (D-ILs), for more efficient CO_2 capture processes when working with commercial packed columns. The energy consumption documented by literature in table 5 was reported in terms of heat energy E_T ($MJ_{th} \cdot kgCO_2^{-1}$). For comparison purpose with the energy consumption results in table 4, the energy consumption of heating regeneration was calculated based on electric energy E_T ($MJ_e \cdot kgCO_2^{-1}$) as expressed in equation 6.

Comparing table 4 and table 5, the MVR technology could decrease the regeneration energy consumption by approximately 30% mainly due to the lower process temperature required for solvent regeneration, which decrease the sensible heat Q_{sens} as discussed in the Methodology section (2.2.). From the absorbent-selection point of view in both approaches, the IL-based regeneration energy consumptions are lower compared to other existing solvent-based technologies for CO_2 capture such as amine- based or aqueous ammonia processes. This could be explained by the lower reaction enthalpy values of the IL studied (from -19 to -39 kJ·mol^{-1}) compared to MEA (−85 kJ·mol^{-1}), which result in higher energy consumption to desorb CO_2 from the amine-based process. Moreover, the use of ILs as absorbents brings some advantages such as negligible solvent loss and may contribute to minimize or to avoid any corrosion and degradation issues that take place in conventional solvent-based process.

Table 5. Comparison of the total energy consumption in CO_2 desorption processes based on conventional flash or stripper column regeneration unit.

Reference	Absorbent and method	ET (MJ_{th}·$kgCO_2^{-1}$)	ET (MJ_e·$kgCO_2^{-1}$)
Abu-Zahra et al. (2007) [63]	MEA solution; Stripper column; 380-410 K; 0.9-2.1 bar	3.0-3.9	1.2-1.5
Yu et al. (2014) [64]	Aqueous ammonia; Stripper column; 363-423 K; 3-8.5 bar	4.0-8.0	1.6-3.2
Khonkaen et al. (2014) [65]	[emim][Ac]; Flash unit, 354 K; 1 bar	2.3	0.9
Shiflett et al. (2010)[66]	[bmim][Ac]; Flash unit, 344 K; 1 bar	2.3	0.9

Taking into account the discussed CO_2 desorption processes alternatives, the combination of the MVR technology and the use of ILs as absorbents is proposed as the most favorable in terms of energy consumption to a conventional thermal regeneration process for its further implementation to large scale applications, due to the lower desorption temperature for CO_2 membrane stripping by using MVR technology compared to the conventional thermal

regeneration, and the advantages of using non-volatile and tunable ILs instead of amine based solvents. However, a detailed techno-economic evaluation is still needed to validate the competitiveness of the HFMC technology by analyzing the difference in costs associated with the large-scale application.

4. Conclusions

In this work, COSMO-based/Aspen Plus methodology have been implemented to the modelling and simulation of CO_2 desorption process using both HFMC technology and ILs as absorbents. A validated 2D-mathematical model developed in our previous work was integrated/exported from ACM into Aspen Plus simulator since there is no HFMC unit in the Aspen Plus model library. The use of the physical property models, the combination of HFMC technology with other unit operations and the process optimization can be performed in Aspen Plus, considering the energy consumption, operational limitations, total costs, and/or process performance requirements. The use of COSMOSAC model provides the capacity to estimate the thermodynamic properties of the pure ILs and CO_2-ILs mixtures. As a result, simulations were performed to evaluate the HFMC operation unit related to the incorporation into the Aspen Plus of the ILs as pseudo-components.

An experimental validation of COSMO-based/Aspen plus modelling and simulation of CO_2 desorption from CO_2-rich IL by membrane contactors was carried out using pure imidazolium ionic liquid [emim][Ac], [bmim][Ac], [bmim][GLY] and [bmim][i-but]. In this context, CO_2 solubility, viscosity and enthalpy of the CO_2-IL chemical reaction were defined as key properties as CO_2 chemical absorbent. The trend in terms of higher efficiency at the same

operational conditions results as follows: [emim][Ac] > [bmim][Ac] > [bmim][i-but] > [bmim][GLY]. Furthermore, the effect on the CO_2 desorption performance and the CO_2 desorption molar flux of the operational conditions: liquid flow-rate, temperature, vacuum pressure and module length were analyzed. On the one hand, high temperature, vacuum level and module length are beneficial to the CO_2 desorption process performance and high CO_2 desorption flux are possible. On the other hand, low liquid flow-rate increases the CO_2 desorption flux but also decrease the efficiency of the regeneration process. Modelling and simulation of the desorption process may allow the optimization of the fluxes and efficiencies of CO_2 recovery under technical conditions. As result, some operational limitations must be analyzed, such as thermal degradation of the membrane, wetting phenomena, fouling or the increase of energy consumption, which lead to a higher overall cost.

The energy consumptions to desorb CO_2 from the CO_2-rich IL by HFMC was evaluated at various operation conditions of temperature and vacuum pressure. The total energy for [emim][Ac] to reach a 90% desorption efficiency is about 0.62 $MJ \cdot kgCO_2^{-1}$, which is much lower to that used conventional high temperature regeneration process (1.55 $MJ \cdot kgCO_2^{-1}$). However, although MVR technology with IL seems to be a promising alternative to large stripping columns in the industrial scale applications, which have been reported higher energy consumption (around 30% higher), some important challenges for the scale-up of this HFMC technology have been identified [67]: (i) prevent wetting phenomena of the membrane which decreases the process efficiency significantly; (ii) increase the operational time capacity by the development of long-term stability membranes or easy-replaceable low-cost membranes; (iii) use environmental friendly absorbents, keeping both high CO_2 solubility and selectivity and (iv) evaluate multi-component streams effects in the carbon capture process efficiency.

Since IL-based HFMC technology is presented as an alternative for CO_2 desorption process rather than thermal regeneration by using packed column configuration, future developments of this technology should focus on: (i) modelling the solvent regeneration process by taking into account adiabatic operating conditions and considering an overall perspective of the continuous absorption-desorption plant in order to study ILs role in equipment investment and operating cost; (ii) finding of new potential ILs overcoming the thermodynamic limitations of the imidazolium ILs studied in this work by COSMO-RS screening, which provide the operational capacity to evaluate or to predict the CO_2 desorption performance with any ILs.

CRediT authorship contribution statement

Jose Manuel Vadillo: Investigation, Conceptualization, Validation, Formal analysis, Data curation, Writing - original draft. **Daniel Hospital-Benito:** Investigation, Writing - review & editing. **Cristian Moya:** Investigation, Writing - review & editing. **Lucia Gomez-Coma:** Supervision, Methodology, Writing - review & editing. **Jose Palomar:** Conceptualization, Methodology, Writing - review & editing. **Aurora Garea:** Conceptualization, Methodology, Writing - review & editing, Funding acquisition. **Angel Irabien:** Supervision, Conceptualization, Project administration, Writing - review & editing.

Notes

1. The equations and procedures of the COSMO-RS method, the custom desorption model (Aspen Custom Modeler) and the simulation (Aspen Plus) files are available under request via correspondence email: vadillojm@unican.es.
2. Nomenclature is fully described in Supplementary Material file.

3. The authors declare that they have no known competing financial interests or personal relationships that could have appeared to influence the work reported in this paper.

Acknowledgements

This work was funded by the Spanish Ministry of Economy, Industry and Competitiveness (MINECO), project CTQ2016-76231-C2-(AEI/FEDER, UE) and project PID2019-108136RB-C31/ AEI / 10.13039/501100011033). J.M.V. thanks the Concepción Arenal postgraduate research grant from the University of Cantabria.

5. References

[1] IEA, The role of CCUS in low-carbon power systems, IEA, Paris. (2020). https://www.iea.org/reports/the-role-of-ccus-in-low-carbon-power-systems (accessed June 24, 2021).

[2] S. Qazi, J. Manuel Vadillo, L. Gómez-Coma, J. Albo, S. Druon-Bocquet, A. Irabien, J. Sanchez-Marcano, CO_2 Capture with Room Temperature Ionic Liquids; Coupled Absorption/Desorption and Single Module Absorption in Membrane Contactor, Chem. Eng. Sci. 223 (2020) 115719. doi:10.1016/j.ces.2020.115719.

[3] J.L. Li, B.H. Chen, Review of CO_2 absorption using chemical solvents in hollow fiber membrane contactors, Sep. Purif. Technol. 41 (2005) 109–122. doi:10.1016/j.seppur.2004.09.008.

[4] Q. Sohaib, A. Muhammad, M. Younas, M. Rezakazemi, Modeling pre-combustion CO_2 capture with tubular membrane contactor using ionic liquids at elevated temperatures, Sep. Purif. Technol. 241 (2020) 116677. doi:10.1016/j.seppur.2020.116677.

[5] J.M. Vadillo, L. Gomez-Coma, A. Garea, A. Irabien, Hollow Fiber Membrane Contactors in CO_2 Desorption : A Review, Energy & Fuels. 35 (2021) 111–136. doi:10.1021/acs.energyfuels.0c03427.

[6] A. Arabi, M. Rezakazemi, F. Seidi, H. Riazi, T. Aminabhavi, M. Soroush, Next generation polymers of intrinsic microporosity with tunable moieties for ultrahigh

permeation and precise molecular CO_2 separation, Prog. Energy Combust. Sci. 84 (2021) 100903. doi:10.1016/j.pecs.2021.100903.

[7] M. Younas, T. Tahir, C. Wu, S. Farrukh, Q. Sohaib, A. Muhammad, M. Rezakazemi, J. Li, Post-combustion CO_2 capture with sweep gas in thin film composite (TFC) hollow fiber membrane (HFM) contactor, J. CO2 Util. 40 (2020) 101266. doi:10.1016/j.jcou.2020.101266.

[8] H. Nieminen, L. Järvinen, V. Ruuskanen, A. Laari, T. Koiranen, J. Ahola, Insights into a membrane contactor based demonstration unit for CO_2 capture, Sep. Purif. Technol. 231 (2020) 115951. doi:10.1016/j.seppur.2019.115951.

[9] J.M. Vadillo, L. Gómez-coma, A. Garea, A. Irabien, CO_2 Desorption Performance from Imidazolium Ionic Liquids by Membrane Vacuum Regeneration Technology, Membranes (Basel). 10 (2020) 234. doi:doi:10.3390/membranes10090234.

[10] N. Intan Listiyana, Y. Rahmawati, S. Nurkhamidah, H. Rofiq Syahnur, Y. Zaelana, CO_2 desorption from activated DEA using membrane contactor with vacuum regeneration technology, MATEC Web Conf. 156 (2018). doi:10.1051/matecconf/201815608012.

[11] Q. He, J. Xi, W. Wang, L. Meng, S. Yan, CO_2 absorption using biogas slurry : Recovery of absorption performance through CO_2 vacuum regeneration, Int. J. Greenh. Gas Control. 58 (2017) 103–113. doi:10.1016/j.ijggc.2017.01.010.

[12] H.J. Lee, M.K. Kim, J.H. Park, Decompression stripping of carbon dioxide from rich monoethanolamine through porous hydrophobic modified ceramic hollow fiber membrane contactor, Sep. Purif. Technol. 236 (2020) 116304. doi:10.1016/j.seppur.2019.116304.

[13] A. Rosli, N.F. Shoparwe, A.L. Ahmad, S.C. Low, J.K. Lim, Dynamic modelling and experimental validation of CO_2 removal using hydrophobic membrane contactor with different types of absorbent, Sep. Purif. Technol. 219 (2019) 230–240. doi:10.1016/j.seppur.2019.03.030.

[14] K. Friess, P. Iz, K. Magda, M. Pasichnyk, M. Lanˇ, D. Nikolaeva, P. Luis, J.C. Jansen, A Review on Ionic Liquid Gas Separation Membranes, (2021).

[15] I. Khan, Q. Sohaib, S. Cao, M. Younas, D. Liu, J. Gui, M. Rezakazemi, Protic / aprotic

ionic liquids for effective CO_2 separation using supported ionic liquid membrane, Chemosphere. 267 (2021) 128894. doi:10.1016/j.chemosphere.2020.128894.

[16] Z. Dai, R.D. Noble, D.L. Gin, X. Zhang, L. Deng, Combination of ionic liquids with membrane technology: A new approach for CO_2 separation, J. Memb. Sci. 497 (2016) 1–20. doi:10.1016/j.memsci.2015.08.060.

[17] L. Bai, S. Zeng, J. Han, B. Yang, L. Deng, H. Gao, X. Zhang, X. Zhang, S. Zhang, Ionic Liquid–Based Membranes for CO_2 Separation, Elsevier Inc., 2018. doi:10.1016/B978-0-12-813645-4.00008-8.

[18] L. Gómez-Coma, A. Garea, A. Irabien, Non-dispersive absorption of CO_2 in [emim][EtSO4] and [emim][Ac]: Temperature influence, Sep. Purif. Technol. 132 (2014) 120–125. doi:10.1016/j.seppur.2014.05.012.

[19] L. Gomez-Coma, A. Garea, A. Irabien, Carbon dioxide capture by [emim][Ac] ionic liquid in a polysulfone hollow fiber membrane contactor, Int. J. Greenh. Gas Control. 52 (2016) 401–409. doi:10.1016/j.ijggc.2016.07.019.

[20] J. Albo, P. Luis, A. Irabien, Carbon dioxide capture from flue gases using a cross-flow membrane contactor and the ionic liquid 1-ethyl-3-methylimidazolium ethylsulfate, Ind. Eng. Chem. Res. 49 (2010) 11045–11051. doi:10.1021/ie1014266.

[21] C.F. Martins, L.A. Neves, R. Chagas, L.M. Ferreira, C.. A.M. Afonso, I.M. Coelhoso, J.G. Crespo, J.P.B. Mota, Modelling CO_2 absorption in aqueous solutions of cholinium lysinate ionic liquid, Chem. Eng. J. (2020) 127875. doi:10.1016/j.cej.2020.127875.

[22] C.F. Martins, L.A. Neves, R. Chagas, L.M. Ferreira, C.A.M. Afonso, J.G. Crespo, CO_2 removal from anaesthesia circuits using gas-ionic liquid membrane contactors, Sep. Purif. Technol. 250 (2020) 116983. doi:10.1016/j.seppur.2020.116983.

[23] T. Mulukutla, G. Obuskovic, K.K. Sirkar, Novel scrubbing system for post-combustion CO_2 capture and recovery: Experimental studies, J. Memb. Sci. 471 (2014) 16–26. doi:10.1016/j.memsci.2014.07.037.

[24] S. Bazhenov, A. Malakhov, D. Bakhtin, V. Khotimskiy, G. Bondarenko, V. Volkov, M. Ramdin, T.J.H. Vlugt, A. Volkov, CO_2 stripping from ionic liquid at elevated pressures in gas-liquid membrane contactor, Int. J. Greenh. Gas Control. 71 (2018) 293–302.

doi:10.1016/j.ijggc.2018.03.001.

[25] J.G. Lu, C.T. Lu, Y. Chen, L. Gao, X. Zhao, H. Zhang, Z.W. Xu, CO_2 capture by membrane absorption coupling process: Application of ionic liquids, Appl. Energy. 115 (2014) 573–581. doi:10.1016/j.apenergy.2013.10.045.

[26] T.J. Simons, P. Hield, S.J. Pas, A novel experimental apparatus for the study of low temperature regeneration CO_2 capture solvents using hollow fibre membrane contactors, Int. J. Greenh. Gas Control. 78 (2018) 228–235. doi:10.1016/j.ijggc.2018.08.009.

[27] S. Qazi, L. Gómez-Coma, J. Albo, S. Druon-Bocquet, A. Irabien, J. Sanchez-Marcano, CO_2 capture in a hollow fiber membrane contactor coupled with ionic liquid: Influence of membrane wetting and process parameters, Sep. Purif. Technol. 233 (2020) 115986. doi:10.1016/j.seppur.2019.115986.

[28] Q. Sohaib, A. Muhammad, M. Younas, M. Rezakazemi, S. Druon-Bocquet, J. Sanchez-Marcano, Rigorous non-isothermal modeling approach for mass and energy transport during CO_2 absorption into aqueous solution of amino acid ionic liquids in hollow fiber membrane contactors, Sep. Purif. Technol. 254 (2021) 117644. doi:10.1016/j.seppur.2020.117644.

[29] Q. Sohaib, J.M. Vadillo, L. Gómez-Coma, J. Albo, S. Druon-Bocquet, A. Irabien, J. Sanchez-Marcano, Post-combustion CO_2 capture by coupling [emim] cation based ionic liquids with a membrane contactor; Pseudo-steady-state approach, Int. J. Greenh. Gas Control. 99 (2020) 103076. doi:10.1016/j.ijggc.2020.103076.

[30] D. Hospital-Benito, J. Lemus, C. Moya, R. Santiago, J. Palomar, Process analysis overview of ionic liquids on CO_2 chemical capture, Chem. Eng. J. 390 (2020) 124509. doi:10.1016/j.cej.2020.124509.

[31] E. Soroush, M. Mesbah, N. Hajilary, M. Rezakazemi, ANFIS modeling for prediction of CO_2 solubility in potassium and sodium based amino acid Salt solutions, J. Environ. Chem. Eng. 7 (2019) 102925. doi:10.1016/j.jece.2019.102925.

[32] A.H. Monjezi, M. Mesbah, M. Rezakazemi, Prediction bubble point pressure for CO_2 / CH_4 gas mixtures in ionic liquids using intelligent approaches, Emergent Mater. 4 (2021) 565–578.

[33] A. Dashti, H. Riasat, M. Rezakazemi, S. Shirazian, Estimating CH_4 and CO_2 solubilities in ionic liquids using computational intelligence approaches, J. Mol. Liq. 271 (2018) 661–669. doi:10.1016/j.molliq.2018.08.150.

[34] J. Palomar, M. Larriba, J. Lemus, D. Moreno, R. Santiago, C. Moya, J. De Riva, G. Pedrosa, Demonstrating the key role of kinetics over thermodynamics in the selection of ionic liquids for CO_2 physical absorption, Sep. Purif. Technol. 213 (2019) 578–586. doi:10.1016/j.seppur.2018.12.059.

[35] A.R.M. Monia, G. Sharma, S.P. Pinho, R.L. Gardas, J.A.P. Coutinho, P.J. Carvalho, Selection and characterization of non-ideal ionic liquids mixtures to be used in CO_2 capture, Fluid Phase Equilib. 518 (2020) 112621. doi:10.1016/j.fluid.2020.112621.

[36] X. Zhang, X. Zhang, H. Dong, Z. Zhao, Y. Huang, Carbon capture with ionic liquids: overview and progress, Energy Environ. Sci. (2012) 6668–6681. doi:10.1039/c2ee21152a.

[37] V.R. Ferro, C. Moya, D. Moreno, R. Santiago, J. De Riva, G. Pedrosa, M. Larriba, I. Diaz, J. Palomar, Enterprise Ionic Liquids Database (ILUAM) for Use in Aspen ONE Programs Suite with COSMO-Based Property Methods, Ind. Eng. Chem. Res. 57 (2018) 980–989. doi:10.1021/acs.iecr.7b04031.

[38] F. Zareiekordshouli, A. Lashanizadehgan, P. Darvishi, Experimental and theoretical study of CO_2 solubility under high pressure conditions in the ionic liquid 1-ethyl-3-methylimidazolium acetate, J. Supercrit. Fluids. 133 (2018) 195–210. doi:10.1016/j.supflu.2017.10.008.

[39] M.B. Shiflett, A. Yokozeki, Phase behavior of carbon dioxide in ionic liquids: [emim][acetate], [emim][trifluoroacetate], and [emim][acetate] + [emim][trifluoroacetate] mixtures, J. Chem. Eng. Data. 54 (2009) 108–114. doi:10.1021/je800701j.

[40] D. Morgan, L. Ferguson, P. Scovazzo, Diffusivities of gases in room-temperature ionic Liquids: Data and correlations obtained using a lag-time technique, Ind. Eng. Chem. Res. 44 (2005) 4815–4823. doi:10.1021/ie048825v.

[41] P. García-Gutiérrez, J. Jacquemin, C. McCrellis, I. Dimitriou, S.F.R. Taylor, C.

Hardacre, R.W.K. Allen, Techno-Economic Feasibility of Selective CO_2 Capture Processes from Biogas Streams Using Ionic Liquids as Physical Absorbents, Energy and Fuels. 30 (2016) 5052–5064. doi:10.1021/acs.energyfuels.6b00364.

[42] J. Elhajj, M. Al-Hindi, F. Azizi, A review of the absorption and desorption processes of carbon dioxide in water systems, Ind. Eng. Chem. Res. 53 (2014) 2–22. doi:10.1021/ie403245p.

[43] F. Ahmad, K.K. Lau, S.S.M. Lock, S. Rafiq, A. Ullah, M. Lee, Hollow fiber membrane model for gas separation : Process simulation , experimental validation and module characteristics study, J. Ind. Eng. Chem. 21 (2014) 1246–1257. doi:10.1016/j.jiec.2014.05.041.

[44] G. Díaz-Sainz, M. Alvarez-Guerra, J. Solla-Gullón, L. García-Cruz, V. Montiel, A. Irabien, Catalyst coated membrane electrodes for the gas phase CO_2 electroreduction to formate, Catal. Today. 346 (2018) 58–64. doi:10.1016/j.cattod.2018.11.073.

[45] Z. Wang, M. Fang, Q. Ma, Z. Zhao, T. Wang, Z. Luo, Membrane stripping technology for CO_2 desorption from CO_2-rich absorbents with low energy consumption, Energy Procedia. 63 (2014) 765–772. doi:10.1016/j.egypro.2014.11.085.

[46] H. Kim, S.J. Hwang, K.S. Lee, Novel Shortcut Estimation Method for Regeneration Energy of Amine Solvents in an Absorption-Based Carbon Capture Process, Environ. Sci. Technol., 49, 1478−1485 (2015). doi:10.1021/es504684x.

[47] N. Matsumiya, M. Teramoto, S. Kitada, H. Matsuyama, Evaluation of energy consumption for separation of CO_2 in flue gas by hollow fiber facilitated transport membrane module with permeation of amine solution, Sep. Purif. Technol. 46 (2005) 26–32. doi:10.1016/j.seppur.2005.04.006.

[48] S. Yan, M. Fang, Z. Luo, K. Cen, Regeneration of CO_2 from CO_2-rich alkanolamines solution by using reduced thickness and vacuum technology: Regeneration feasibility and characteristic of thin-layer solvent, Chem. Eng. Process. 48 (2009) 515–523. doi:10.1016/j.cep.2008.06.009.

[49] D. Albarracin-Zaidiza, B. Belaissaoui, D. Roizard, E. Favre, S. Rode, Stripping of CO_2 in Post-combustion Capture with Chemical Solvents: Intensification Potential of Hollow

Fiber Membrane Contactors, Energy Procedia. 114 (2017) 1334–1341. doi:10.1016/j.egypro.2017.03.1254.

[50] Y. Shen, C. Jiang, S. Zhang, J. Chen, L. Wang, J. Chen, Biphasic solvent for CO_2 capture : Amine property-performance and heat duty relationship, Appl. Energy. 230 (2018) 726–733. doi:10.1016/j.apenergy.2018.09.005.

[51] R. Wang, L. Jiang, Q. Li, G. Gao, S. Zhang, L. Wang, Energy-saving CO_2 capture using sulfolane-regulated biphasic solvent, Energy. 211 (2020) 118667. doi:10.1016/j.energy.2020.118667.

[52] D.A. Zaidiza, B. Belaissaoui, S. Rode, E. Favre, Intensification potential of hollow fiber membrane contactors for CO_2 chemical absorption and stripping using monoethanolamine solutions, Sep. Purif. Technol. 188 (2017) 38–51. doi:10.1016/j.seppur.2017.06.074.

[53] M. Fang, Z. Wang, S. Yan, Q. Cen, Z. Luo, CO_2 desorption from rich alkanolamine solution by using membrane vacuum regeneration technology, Int. J. Greenh. Gas Control. 9 (2012) 507–521. doi:10.1016/j.ijggc.2012.05.013.

[54] M.T. Mota-Martinez, J.P. Hallett, N. Mac Dowell, Solvent selection and design for CO_2 capture-how we might have been missing the point, Sustain. Energy Fuels. 1 (2017) 2078–2090. doi:10.1039/c7se00404d.

[55] M.B. Shiflett, B.A. Elliott, S.R. Lustig, S. Sabesan, M.S. Kelkar, A. Yokozeki, Phase behavior of CO_2 in room-temperature ionic liquid 1-ethyl-3-ethylimidazolium acetate, ChemPhysChem. 13 (2012) 1806–1817. doi:10.1002/cphc.201200023.

[56] R. Santiago, J. Lemus, C. Moya, D. Moreno, N. Alonso-Morales, J. Palomar, Encapsulated Ionic Liquids to Enable the Practical Application of Amino Acid-Based Ionic Liquids in CO_2 Capture, ACS Sustain. Chem. Eng. 6 (2018) 14178–14187. doi:10.1021/acssuschemeng.8b02797.

[57] M.I. Cabaço, M. Besnard, Y. Danten, J.A.P. Coutinho, Carbon dioxide in 1-butyl-3-methylimidazolium acetate. I. Unusual solubility investigated by Raman spectroscopy and DFT calculations, J. Phys. Chem. A. 116 (2012) 1605–1620. doi:10.1021/jp211211n.

[58] L. Zhou, X. Shang, J. Fan, J. Wang, Solubility and selectivity of CO_2 in ether-functionalized imidazolium ionic liquids, J. Chem. Thermodyn. 103 (2016) 292–298. doi:10.1016/j.jct.2016.08.028.

[59] J. Palomar, V.R. Ferro, J.S. Torrecilla, F. Rodríguez, Density and molar volume predictions using COSMO-RS for ionic liquids. An approach to solvent design, Ind. Eng. Chem. Res. 46 (2007) 6041–6048. doi:10.1021/ie070445x.

[60] M. Fang, Z. Wang, S. Yan, Q. Cen, Z. Luo, CO_2 desorption from rich alkanolamine solution by using membrane vacuum regeneration technology, Int. J. Greenh. Gas Control. 9 (2012) 507–521. doi:10.1016/j.ijggc.2012.05.013.

[61] D. Hospital-Benito, J. Lemus, R. Santiago, J. Palomar, Thermodynamic and kinetic evaluation of ionic liquids + tetraglyme mixtures on CO_2 capture, J. CO2 Util. 35 (2020) 185–193. doi:10.1016/j.jcou.2019.09.015.

[62] W.T. Zheng, F. Zhang, Y.T. Wu, X.B. Hu, Concentrated aqueous solutions of protic ionic liquids as effective CO_2 absorbents with high absorption capacities, J. Mol. Liq. 243 (2017) 169–177. doi:10.1016/j.molliq.2017.08.035.

[63] M.R.M. Abu-Zahra, L.H.J. Schneiders, J.P.M. Niederer, P.H.M. Feron, G.F. Versteeg, CO_2 capture from power plants. Part I. A parametric study of the technical performance based on monoethanolamine, Int. J. Greenh. Gas Control. 1 (2007) 37–46. doi:10.1016/S1750-5836(06)00007-7.

[64] J. Yu, S. Wang, H. Yu, L. Wardhaugh, P. Feron, Rate-based modelling of CO_2 regeneration in ammonia based CO_2 capture process, Int. J. Greenh. Gas Control. 28 (2014) 203–215. doi:10.1016/j.ijggc.2014.06.032.

[65] K. Khonkaen, K. Siemanond, A. Henni, Simulation of carbon dioxide capture using ionic liquid 1-Ethyl-3-methylimidazolium Acetate, Elsevier, 2014. doi:10.1016/B978-0-444-63455-9.50009-X.

[66] M.B. Shiflett, D.W. Drew, R.A. Cantini, A. Yokozeki, Carbon dioxide capture using ionic liquid 1-butyl-3-methylimidazolium acetate, Energy and Fuels. 24 (2010) 5781–5789. doi:10.1021/ef100868a.

[67] P. Luis, T. Van Gerven, B. Van Der Bruggen, Recent developments in membrane-based

technologies for CO_2 capture, Prog. Energy Combust. Sci. 38 (2012) 419–448. doi:10.1016/j.pecs.2012.01.004.

GRAPHICAL ABSTRACT

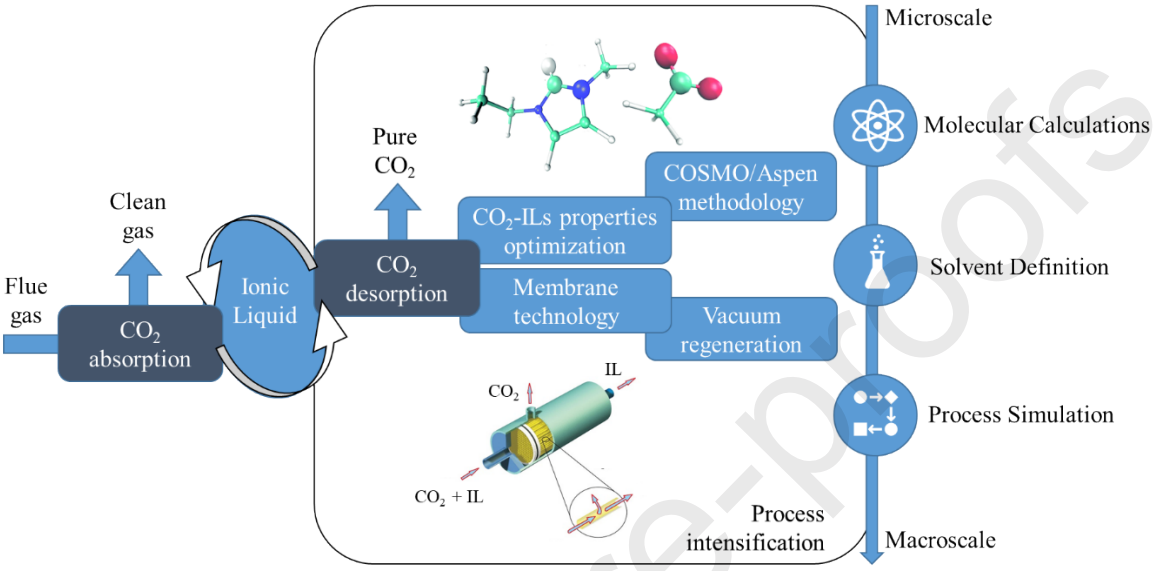

CRediT authorship contribution statement

Jose Manuel Vadillo: Investigation, Conceptualization, Validation, Formal analysis, Data curation, Writing - original draft. **Daniel Hospital-Benito:** Investigation, Writing - review & editing. **Cristian Moya:** Investigation, Writing - review & editing. **Lucia Gomez-Coma:** Supervision, Methodology, Writing - review & editing. **Jose Palomar:** Conceptualization, Methodology, Writing - review & editing. **Aurora Garea:** Conceptualization, Methodology, Writing - review & editing, Funding acquisition. **Angel Irabien:** Supervision, Conceptualization, Project administration, Writing - review & editing.

Declaration of interests

☒ The authors declare that they have no known competing financial interests or personal relationships that could have appeared to influence the work reported in this paper.

☐The authors declare the following financial interests/personal relationships which may be considered as potential competing interests: